NASA Technical Paper 1629

Simulation Study of a Geometric Shape Factor Technique for Estimating Earth-Emitted Radiant Flux Densities From Wide-Field-of-View Radiation Measurements

William L. Weaver and Richard N. Green

APRIL 1980

NASA

NASA Technical Paper 1629

Simulation Study of a Geometric Shape Factor Technique for Estimating Earth-Emitted Radiant Flux Densities From Wide-Field-of-View Radiation Measurements

William L. Weaver and Richard N. Green
Langley Research Center
Hampton, Virginia

National Aeronautics
and Space Administration

**Scientific and Technical
Information Office**

1980

SUMMARY

A study was performed on the use of geometric shape factors to estimate Earth-emitted radiant flux densities from radiation measurements made with wide-field-of-view radiometers on satellites. Sets of simulated irradiance measurements were computed for unrestricted- and restricted-field-of-view, wide-angle detectors. The study emphasized horizontal flat-plate detectors, but spherical detectors were also considered. In these simulations, data from the Nimbus 2 and 3 satellites were used to model the Earth's long-wave radiation field. Geometric shape factors were derived and applied to these data to estimate flux densities over a reference surface. These flux density estimates were calculated for global and zonal scales and for areas smaller than the detector field of view (FOV). For measurements at a satellite altitude of 600 km, estimates of zonal flux density were in error 1.0 to 1.2 percent, and estimates of global flux density were in error less than 0.2 percent. Estimates with unrestricted-field-of-view (UFOV) detectors were about the same for Lambertian and limb-darkening radiation models but were affected by satellite altitude. The opposite was found for the restricted-field-of-view detectors. The UFOV detector is a poor estimator of flux density from its total FOV and performs better as an estimator of flux density from a circle centered at the FOV with an area significantly smaller than that for the total FOV.

INTRODUCTION

Solar energy plays the dominant role in generating the Earth's weather and climate. Research to improve our understanding of this role has increased significantly with advances in Earth satellite technology because modern satellites have proven to be excellent platforms from which to monitor the amounts of solar energy that the Earth reflects, absorbs, and emits. There are two major classes of radiometers in use on satellites to monitor this radiant energy: wide-field-of-view (WFOV) radiometers, and narrow-field-of-view scanning radiometers. Both classes of radiometers have seen extensive duty in meteorological and climate research since the meteorological satellite TIROS II was launched in 1960. This paper deals with the study of a technique to analyze measurements from WFOV detectors.

A WFOV radiometer integrates radiation from a very large region of the Earth and its atmosphere. At an altitude of 600 km, for instance, an unrestricted-field-of-view (UFOV) detector has a circular Earth field of view (FOV) with a diameter of about 5000 km; thus, one could directly obtain a good estimate of the global flux from a large set of globally uniform radiation measurements made with a UFOV flat-plate detector. Global sets of radiation measurements made from satellites, however, are not completely uniform in time and space, and statistical weighting of the measurements must be applied to obtain estimates of global flux. Analytical techniques can be applied to both restricted and unrestricted FOV radiation measurements to obtain estimates of radiant flux densities on smaller spatial scales. Because of their measurement

capability and because they are simpler and more operationally reliable than narrow-field-of-view scanning radiometers, WFOV radiometers are assured of a continuing role in satellite-borne radiation measurement experiments. WFOV radiometers are part of the ERB (Earth Radiation Budget) Experiment aboard the Nimbus 6 and Nimbus 7 satellites and will be included in the Earth Radiation Budget Experiment (ERBE) proposed for launch in the mid 1980's (refs. 1 and 2).

Two basic techniques can be employed to analyze WFOV radiation measurements. One technique involves using a parameter estimation technique which was developed in references 3 and 4. This paper studies another technique which is a simpler and more direct approach that uses geometric shape factors to relate WFOV Earth-emitted radiation measurements to estimates of flux densities on global and smaller scales. With this technique, an estimate of average flux density at a reference surface is realized for each irradiance measurement at the satellite by simply multiplying the measurement by a geometric shape factor. The shape factor is computed by assuming that the emitted radiant flux density is constant over the reference surface everywhere within the detector FOV.

The purpose of this study is to evaluate the effects of this assumption when the shape factor technique is used to estimate average flux densities on global and zonal scales and for the individual measurements. To do this, a computer program was employed to generate sets of simulated Earth-emitted radiation measurements which might be obtained with WFOV radiometers on a satellite. The model of the Earth-emitted flux density field employed in the simulation program was based on data from the Nimbus 2 and 3 satellites (ref. 5). Some simulated measurement sets were made assuming the radiation field to be Lambertian and others were made in which the field was modified by a limb-darkening function. Unrestricted and restricted FOV horizontal flat-plate and UFOV spherical detectors were studied. Particular emphasis was put on the plate detectors because all current (Nimbus 6 and 7, for instance) and near-future (ERBE) detectors are of this type. Geometric shape factors were applied to the simulated measurements to produce estimates of average emitted flux density on different spatial scales. These estimates are then compared with reference averages derived directly from the flux density model. The shape factor concept is derived in this paper, and the shape factors employed are seen to depend only on the maximum FOV of the detector.

NOMENCLATURE

A	area, m^2
A_G	global area, m^2
AME	average measurement error, percent
AZE	average zonal error, percent
E	irradiance measurement at satellite, W/m^2

ECA	Earth central angle subtended by diameter of detector Earth field of view, deg
F	geometric shape factor, dimensionless
FOV	field of view, deg
GE	global error, percent
h	satellite altitude, km
ℓ	distance (fig. 2), m
L	radiance, W/m^2-sr
M	flux density, or exitance, at top of Earth atmosphere, W/m^2
r	radius to top of atmosphere, same as radius of Earth for this study, 6378 km
R	radiance directional model, dimensionless
RFOV	restricted field of view (ECA = 20^o)
S	radiometer response function, dimensionless
UFOV	unrestricted field of view
WFOV	wide field of view (includes UFOV and RFOV)
θ_m	cone angle of detector Earth FOV as seen from satellite, deg
λ,ϕ	longitude, latitude (fig. 1), deg
θ,ψ	coordinates at satellite (fig. 1), deg
ψ',τ	angular directions of radiation component, deg
Ω	solid angle, sr
$(\bar{})$	reference average of quantity derived from model
$(\hat{})$	estimate of quantity

Subscript:

j	zonal value

SHAPE FACTOR CONCEPT FOR EARTH-EMITTED RADIATION

The Earth's long-wave radiance field L on a reference surface above the Earth is defined as a function of Earth position (longitude λ and latitude ϕ) and the emission direction (ray azimuth ψ' and ray zenith τ). The long-wave radiance is confined to wavelengths longer than 5 μm and is considered constant with time. An increment of irradiance dE sensed by a WFOV detector aboard an Earth satellite (see fig. 1) can be related to the Earth radiance field by

$$dE = L(\lambda,\phi,\psi',\tau)\ S(\theta,\psi)\ d\Omega \tag{1}$$

where S is the radiometer response and is a function of the cone angle θ and the azimuth angle ψ; $d\Omega$ is the solid angle at the satellite subtended by the increment of surface area dA. A directional function R can be defined such that the radiance can be expressed as a product of the directional function and the flux density M; that is,

$$L(\lambda,\phi,\psi',\tau) = \frac{1}{\pi} M(\lambda,\phi)\ R(\lambda,\phi,\psi',\tau)$$

where R is normalized by

$$\frac{1}{\pi}\int_{\psi'=0}^{2\pi}\int_{\tau=0}^{\pi/2} R(\lambda,\phi,\psi',\tau)\ \sin\psi'\ \cos\psi'\ d\psi'\ d\tau = 1$$

If the solid angle is expressed in terms of coordinates at the satellite $d\Omega = \sin\theta\ d\theta\ d\psi$, the total irradiance sensed by the detector at the satellite can be written as the integral of equation (1) over the detector field of view, or

$$E = \frac{1}{\pi}\int_{\psi=0}^{2\pi}\int_{\theta=0}^{\theta_m} M(\lambda,\phi)\ R(\psi,\phi,\psi',\tau)\ S(\theta,\psi)\ \sin\theta\ d\theta\ d\psi \tag{2}$$

where θ_m defines the limit of the field of view on the reference surface. One way of solving this equation for the flux density is to assume that the flux density is uniform over the field of view. Then equation (2) reduces to

$$E = \frac{M}{\pi}\int_{\psi=0}^{2\pi}\int_{\theta=0}^{\theta_m} R(\lambda,\phi,\psi',\tau)\ S(\theta,\psi)\ \sin\theta\ d\theta\ d\psi$$

or

$$M = F^{-1}E$$

where F is the geometric shape factor given by

$$F = \frac{1}{\pi} \int_{\psi=0}^{2\pi} \int_{\theta=0}^{\theta_m} R(\lambda,\phi,\psi',\tau)\ S(\theta,\psi)\ \sin\theta\ d\theta\ d\psi \qquad (3)$$

Thus, given a measurement of irradiance at a satellite, there is a corresponding realization of a flux density at the reference surface.

The physical interpretation of the shape factor is the detector response to a uniform radiance field, where $M(\lambda,\phi) = 1$. Moreover, if the radiance at the reference surface is everywhere independent of direction of emission; that is, if the radiance emitted into a unit solid angle is equal in all directions, then the radiance is Lambertian and $R(\lambda,\phi,\psi',\tau) = 1$. With these assumptions the shape factor can be determined for a flat-plate detector, where $S(\theta,\psi) = \cos\theta$, and for a spherical detector, where $S(\theta,\psi) = 1$, by integrating equation (3) to obtain

$$\left.\begin{aligned} F &= \sin^2\theta_m \qquad \text{(Flat plate)} \\ F &= 2(1 - \cos\theta_m) \qquad \text{(Sphere)} \end{aligned}\right\} \text{Lambertian assumption} \qquad \begin{aligned} &(4a) \\ &(4b) \end{aligned}$$

For a UFOV detector, θ_m is a function only of the radius r to the reference surface (usually taken as the top of the atmosphere) and the altitude h above the reference surface:

$$\theta_m = \sin^{-1}\frac{r}{r + h}$$

and therefore the shape factor for a UFOV flat-plate detector reduces to an expression of the inverse-square law for radiation:

$$F = \left(\frac{r}{r + h}\right)^2$$

This is sometimes referred to as the height rectification factor.

SIMULATION PROGRAM AND RADIATION MODEL

The simulation program employed is the same one described in reference 4. The flux density field is a static model of the Earth-emitted radiation field which was based on results from the Nimbus 2 and 3 data analysis of reference 5. This model is comprised of 1654 discrete values of flux density, each representing an area A_i on the Earth's surface approximately equal to a $5^o \times 5^o$ region at the equator (see fig. 2). Note that the reference surface is the same as the Earth's surface; this amounts to ignoring the thickness of the atmosphere. Two directional functions were employed in the model. The first was Lambertian (R = 1) and the other was the average limb-darkening function based on the analysis of references 4 and 5. This function, which is dependent on the zenith angle τ only, is shown in figure 3.

The simulation program computes a discrete value of irradiance E_i sensed by a WFOV detector from a single discrete region on the Earth of area A_i (see fig. 2) through the equation

$$E_i = \frac{1}{\pi} M_i \, R(\tau_i) \, S(\theta_i) \, \frac{\cos \tau_i A_i}{\ell_i^2} \tag{5}$$

where the solid angle $\sin \theta \, d\theta \, d\psi$ is replaced by the relationship $\cos \tau_i A_i / \ell_i^2$. A total simulated measurement of irradiance is the sum of equation (5) over the detector field of view expressed by

$$E = \frac{1}{\pi} \sum_{i=1}^{N} M_i \, R(\tau_i) \, S(\theta_i) \frac{\cos \tau_i A_i}{\ell_i^2}$$

where N is the number of discrete regions of the model with centers in the detector Earth field of view. The detector response function $S(\theta)$ was either $\cos \theta$ or 1.0, depending on whether the measurements simulated those of a flat plate or a sphere, respectively.

An estimate of flux density $\hat{M}$ from a single simulated irradiance measurement is obtained by

$$\hat{M} = F^{-1} E$$

where the shape factor F is computed by equation (3). The reference flux density is the average taken directly from the model over any area within the detector Earth field of view and is given by

$$\bar{M} = \frac{1}{N} \sum_{m=1}^{N} M_m$$

where N is the number of discrete regions of the model with centers in that given area. Thus, the error in estimating flux density is the difference between $\bar{M}$ and $\hat{M}$.

Global sets of simulated measurements were generated with the program by specifying orbit characteristics, the number of orbits, and measurements per orbit. Measurements were equally spaced along the orbit, and the ascending nodes of the orbits were equally spaced at the equator.

CALCULATIONS AND ANALYSIS

10° Zones and the Globe

All the data sets in the study were generated with circular orbits with an inclination of 100°. Hence, the spatial distributions of the sets are what might be expected from typical Sun-synchronous orbits with no data dropouts. For typical experiments with Sun-synchronous orbits, the number of measurements is substantially higher at the extreme latitudes than in the equatorial regions. This is why the global flux density cannot be determined from a simple average of the measurements in a global data set.

The parameters and their ranges whose effects on estimating zonal and global flux densities were studied are summarized in table I for each of the two types of detectors. The Earth FOV diameter of the RFOV (ECA = 20°) detector was fixed at about 2000 km for all satellite altitudes. For comparison, the Earth FOV diameter of the UFOV detector at an altitude of 600 km is about 5000 km.

An estimate of the average flux density $\hat{M}_j$ in the jth 10° latitude zone is obtained from a global data set by

$$\hat{M}_j = \frac{1}{N} \sum_{m=1}^{N} \hat{M}_m$$

where N is the number of measurement estimates of the set whose centers are in the jth latitude zone. An estimate of the average global flux density $\hat{M}_G$ is obtained by averaging the area-weighted averages in the 18 latitude zones:

$$\hat{M}_G = \frac{1}{A_G} \sum_{j=1}^{18} \hat{M}_j A_j$$

where A_j is the area of the jth zone and A_G is the global area.

The corresponding reference or model values of average flux density in a 10^o zone $\bar{M}_j$ and average global flux density $\bar{M}_G$ were obtained directly from the flux density model. These reference flux densities are given in figure 4 and represent a typical Northern Hemisphere winter day. The global error GE is given by

$$GE = \frac{\hat{M}_G - \bar{M}_G}{\bar{M}_G} \times 100 \tag{6}$$

A figure of merit, the "average zonal error" AZE, was calculated to evaluate the ability of the technique to estimate flux densities from a set of global measurements. The average zonal error is the area-weighted average of the absolute values of zonal errors:

$$AZE = \frac{1}{A_G} \sum_{j=1}^{18} \text{abs}\left(\frac{\hat{M}_j - \bar{M}_j}{\bar{M}_j}\right) A_j \times 100 \tag{7}$$

Figure 5 shows typical results obtained to study how the average zonal error (AZE) is affected by the number of orbits and number of measurements per orbit in a measurement set. These results were calculated from measurements with flat-plate detectors at an altitude of 600 km and a Lambertian radiation model. Geometric shape factors derived by equation (4a) were used to make all the estimates. The actual values of the shape factors used were

For UFOV detectors F = 0.8354

For RFOV detectors F = 0.7163

The minimum values of AZE achieved with 2-orbit or 15-orbit measurement data sets are reached by about 40 or 50 data points per orbit with both the UFOV and RFOV detectors. The minimum values of AZE (about 1.0 to 1.2 percent) achieved with the 15-orbit set were not reduced significantly by increasing the number of orbits to 50. The global errors GE corresponding to the results of figure 5 were less than 0.2 percent when the number of orbits was 15 or more and the number of measurements per orbit was 50 or more.

The effect of satellite altitude on the minimum AZE is shown in figure 6 for flat-plate detectors and a Lambertian radiation model. All the measurement sets were obtained for 15 orbits and 55 measurements per orbit, and the geometric shape factors computed by equation (4a) were used to make all the estimates. The errors are about constant to an altitude of 600 km for both the UFOV and RFOV detectors. The errors remain about constant to 1000 km for the RFOV detector but increase to 2 percent for the UFOV detector. The increase in error with altitude for the UFOV detector indicates a decrease in zonal resolution due to an increase in the Earth FOV. The Earth FOV remains constant with altitude for the RFOV detector. The altitudes considered bracket the expected altitudes for the currently proposed Earth Radiation Budget Satellite system (ref. 2).

For each global measurement set, the simulation program computed a shape factor which minimized AZE (eq. (7)) for the set. The shape factors computed in this manner were nearly the same as those computed by equation (4a) for the measurement sets of figures 5 and 6 with at least 15 orbits and 50 points per orbit. Thus the geometric shape factor is the optimum constant for estimating zonal flux densities from sets of measurements made with flat-plate detectors and a Lambertian radiation model.

Figures 7 to 9 present comparisons between estimated and reference values of average zonal flux densities for some representative measurement sets obtained with flat-plate detectors. Values of reference flux density are derived directly from the flux density model and are the same as those of figure 4. All measurement sets were for a satellite altitude of 600 km and consisted of 15 orbits and 55 measurements per orbit. Shown also in these figures are the computed values of AZE (eq. (7)) and GE (eq. (6)). Figure 7 gives results for a UFOV detector for measurement sets made with the Lambertian and limb-darkening radiation models. Estimates for both measurement sets were made with the UFOV shape factor $F = 0.8354$ shown on page 8. Estimated values of average zonal flux densities made from measurements with both directional models agree well with the reference values. A close inspection reveals that the zonal flux density is overestimated for some zones and underestimated for others. This explains why the global error (eq. (6)) is much smaller than the average zonal error, which is derived by using absolute values of zonal errors (see eq. (7)). Both errors (AZE and GE) are similar for the Lambertian and limb-darkening directional models. It was found, in general, that the computed optimum shape factors for the UFOV detector were independent of the directional model employed in calculating the simulated measurement sets.

Figure 8 shows results from simulated measurements made with RFOV detectors with the Lambertian and limb-darkening directional models. The RFOV shape factor $F = 0.7163$ (shown on page 8) was used to make these estimates. Estimates are about the same as with the UFOV detector (fig. 7) for measurements made with the Lambertian directional function. However, estimates based on measurements made with the limb-darkening function are all seen to be high. The average zonal error (AZE) more than doubled over that for the Lambertian model and the global error (GE) increased to more than 2.0 percent. Thus, the RFOV shape factor derived under the assumption of a Lambertian model (eq. (4a)) produces a bias when used to estimate measurements made with the limb-darkening model.

Figure 9 shows the results obtained when the optimum shape factor computed by the simulation program is used to reduce the limb-darkening measurements of figure 8 to estimates of flux density. Using the optimum shape factor brought the estimate of zonal flux density more into line with those seen for the Lambertian function of figure 8, and AZE and GE are also reduced to about the same order as those of figure 8. An RFOV geometric shape factor was computed from the equation

$$F = \frac{1}{\pi} \int_0^{2\pi} \int_0^{\theta_m} R(\tau) \cos\theta \sin\theta \, d\theta \, d\psi \tag{8}$$

This is equation (3) with

$$R(\lambda,\phi,\psi',\tau) = R(\tau)$$

and

$$S(\theta,\psi) = \cos\theta$$

where $R(\tau)$ is the limb-darkening function of figure 3. This computed geometric shape factor and the optimum shape factor computed by the simulation program are

Computed geometric $F = 0.7354$

Computed optimum $F = 0.7338$

The difference is only 0.2 percent. Thus the geometric shape factor can be used to estimate flux densities from measurements with RFOV flat-plate detectors provided the directional radiation model is known.

UFOV spherical detectors were studied for an altitude of 600 km and a Lambertian radiation model. Estimates of flux density were based on the shape factor computed by equation (4b). The actual value was

$$F = 1.1886$$

As for the UFOV flat-plate detectors, the optimum shape factors computed by the program agreed quite well with the value $F = 1.1886$. Results were similar to those for the UFOV flat-plate detector, but the values of AZE were larger. Results from a typical case with the spherical detector are shown in figure 10. It can be seen that the estimates of zonal flux density are quite

similar to those for the UFOV flat-plate detector (fig. 7). The global error is about the same and AZE is larger.

Areas in Detector Field of View

In the previous section, this study examined the ability of the geometric shape factor method to estimate zonal and global averages of emitted flux density from global sets of simulated irradiance measurements. It is also of interest to study how well a WFOV detector estimates flux density from individual measurements. If a detector measured irradiance equally from all locations in its Earth FOV, then an estimate of flux density based on a single measurement should best represent the average flux density over the total FOV. Figure 11 illustrates the actual irradiance measurement characteristics of UFOV detectors relative to the Earth area within the detector FOV from which the radiance is emitted. The detector altitude is 600 km. The irradiance fraction is that part of the total irradiance which is due to emission from a circular area centered at the detector Earth field of view. The Earth central angle is the angle subtended by the diameter of the circle. The percentage of total area is also shown. One-half the irradiance sensed by the plate detector is due to emission from an area which is only 5 percent of the total, and 9/10 of the irradiance is due to emission from an area about 25 percent of the total area within the detector Earth FOV.

When an estimate of flux density is made from a single measurement with a WFOV flat-plate detector, over what area in the detector FOV does the estimate best represent the actual average flux density? To answer this question, four sets of eight measurements each were made with identical spatial distributions. The altitude was 600 km, latitude was 2.5°, and measurements were equally spaced (45°) in longitude. The four measurement sets differed as follows:

1	UFOV	Lambertian model
2	UFOV	limb-darkening model
3	RFOV	Lambertian model
4	RFOV	limb-darkening model

Estimates of flux density were made for each measurement using a shape factor based on the assumption of a Lambertian radiation model (eq. (4a)). The estimates from each of the four measurement sets were compared with the reference values for several circular areas within the field of view of the detectors. The Earth central angles for these reference areas are

UFOV

$$ECA = 5^{\circ}, 15^{\circ}, 20^{\circ}, 25^{\circ}, 30^{\circ}, 40^{\circ}, 48^{\circ}$$

RFOV

$$ECA = 5^{\circ},\ 15^{\circ},\ 20^{\circ}$$

A figure of merit, the average measurement error (AME), was calculated from

$$(AME)_{\ell k} = \frac{1}{8}\sum_{m=1}^{8} \text{abs}\left(\frac{\hat{M}_{m\ell} - \bar{M}_{mk}}{\bar{M}_{mk}}\right) \times 100$$

where ℓ represents the measurement set on which estimates are based and k represents the area on which the reference values of flux density are based.

Figure 12 shows the resulting values of AME plotted against the values of ECA which correspond to the areas within the detector FOV on which the reference flux densities are based. The UFOV detector gives a poor estimate when measurements are compared with the reference flux density over the total field of view (ECA = 48°). Errors decrease with decreasing ECA, reach a minimum at ECA = 20°, and then increase again with decreasing ECA. Errors are about the same whether the radiation model for the measurements is Lambertian or limb-darkening, a result which is consistent with the zonal analysis (fig. 7). For these limited data, the UFOV detector gives a much better estimate of the flux density from a region which is significantly smaller than the detector total Earth FOV.

The results are not as clear for measurements with the RFOV detector as those for the UFOV detector, but it appears that the estimates are more representative of the flux density over the total FOV (ECA = 20°). The estimates also appear to be no better than those made with the UFOV detector. Errors are larger for measurements based on the limb-darkening function, a result consistent with the zonal analysis (fig. 8).

The results of figure 12 were obtained with sets of measurements which are representative of the flux density near the equator, and the question arises whether they would be valid for a range of latitudes. To investigate possible latitude effects, a set of UFOV measurements was computed every 10° along a 600-km orbit with an inclination of 100°. The UFOV shape factor value $F = 0.8354$ was used to make an estimate of flux density for each measurement. Resulting errors are presented in figure 13. When estimates are compared with reference flux densities for the detector total FOV (circles), errors are seen to oscillate substantially and in some cases to exceed 11 percent. However, when estimates are compared with reference flux density for the reduced FOV (ECA = 20°), errors are reduced in most cases and maximum errors are only one-half of those for the total FOV case.

In reference 6, Vinnikov made a theoretical study of UFOV detectors. He employed a theoretical radiance field which was homogeneous in azimuth ψ and varied with ray zenith τ much as the limb-darkening radiation model of this study. His results indicated that an estimate of flux density based on a

measurement at an altitude of 600 km was representative of the reference flux density for an area significantly smaller than the detector total Earth FOV. The Earth central angle (ECA) of this smaller area was about 15° as compared with 20° for the current study.

CONCLUDING REMARKS

The concept of using geometric shape factors to estimate flux densities from irradiance measurements made with wide-field-of-view flat-plate and spherical detectors on a satellite is described. A simulation program is described and employed to evaluate the effectiveness of the shape factor technique to estimate Earth-emitted flux densities on zonal and global scales. This is done by computing global sets of irradiance measurements typical of those which might be obtained from circular Sun-synchronous orbits. Zonal and global estimates of flux densities were made from the measurement sets and compared with reference values obtained directly from the flux density model. The radiance model was based on data from the Nimbus 2 and 3 satellites.

Minimum errors in zonal and global estimates were achieved with 15 orbits and about 40 to 50 measurements per orbit. Errors were nearly independent of altitude from 300 to 1000 km for the restricted-field-of-view (RFOV) flat-plate detectors but increased between altitudes of 600 and 1000 km for the unrestricted-field-of-view (UFOV) detector. Errors with the UFOV flat-plate detector were about the same for measurements made with Lambertian and limb-darkening radiation directional models. However, a similar comparison with the RFOV flat-plate detector produced significantly higher errors with the limb-darkening model. It was found that these higher errors can be reduced significantly if the directional model is known. Measurements with UFOV spherical detectors were simulated with a Lambertian radiation model only. Average zonal errors were greater and global errors were about the same when compared with errors with UFOV flat-plate detectors.

Simulated measurements were also used to evaluate the effectiveness of estimating average flux density from individual measurements with UFOV and RFOV flat-plate detectors. The UFOV detector is a poor estimator of flux density from its total field of view and performs much better as an estimator of flux density from a circle centered at the detector field of view with an Earth central angle (ECA) of 20°. Little variation was found in estimates with UFOV detectors between measurements made with a Lambertian and a limb-darkening radiation model. Within the ECA = 20° range, the RFOV detector appears to be no more effective than the UFOV detector as an estimator of flux density from individual measurements. Errors increase when the measurements are made with a limb-darkening radiation model.

Langley Research Center
National Aeronautics and Space Administration
Hampton, VA 23665
February 22, 1980

REFERENCES

1. Woerner, Charles V.; and Cooper, John E.: Earth Radiation Budget Satellite System Studies. NASA TM X-72776, 1977.

2. Cooper, John E.; and Woerner, Charles V.: The Earth Radiation Budget Satellite System of the Early 1980's. Fourth Symposium on Meteorological Observations and Instrumentation, American Meteorol. Soc., 1978, pp. 172-178.

3. Smith, G. Louis; and Green, Richard N.: Theoretical Analysis of Wide Field of View Radiometer Measurements of Earth Energy Budget. NASA paper presented at Fifth Annual Remote Sensing of Earth Resources Conference (Tullahoma, Tenn.), Mar. 29-31, 1976.

4. Green, Richard N.: Simulation Studies of Wide and Medium Field of View Earth Radiation Data Analysis. NASA TP-1182, 1978.

5. Raschke, Ehrhard; Vonder Haar, Thomas H.; Bandeen, William R.; and Pasternak, Musa: The Annual Radiation Balance of the Earth-Atmosphere System During 1969-70 From Nimbus 3 Measurements. J. Atmos. Sci., vol. 30, no. 3, Apr. 1973, pp. 341-364.

6. Vinnikov, K. Ja (C. P. Long, transl.): On the Problem of the Interpretation of Measurements of Outgoing Radiation Made by Radiometers With an Unrestricted Field of Vision on Meteorological Satellites of the Earth. Misc. Transl., Ser. M, No. 7853, Natl. Lending Libr. Sci. & Technol. (Boston Spa, England), [1968].

TABLE I.- PARAMETERS AND RANGES STUDIED FOR FLAT-PLATE AND SPHERICAL DETECTORS

Parameter	Range of parameter for -	
	Flat-plate detector	Spherical detector
Field of view	UFOV (horizon-to-horizon) RFOV (ECA = 20°)	UFOV (horizon-to-horizon)
Number of orbits	1 to 50	15
Measurements per orbit	9 to 100	9 to 72
Satellite altitude, km	300 to 1000	600
Radiation directional models	Lambertian Limb-darkening	Lambertian

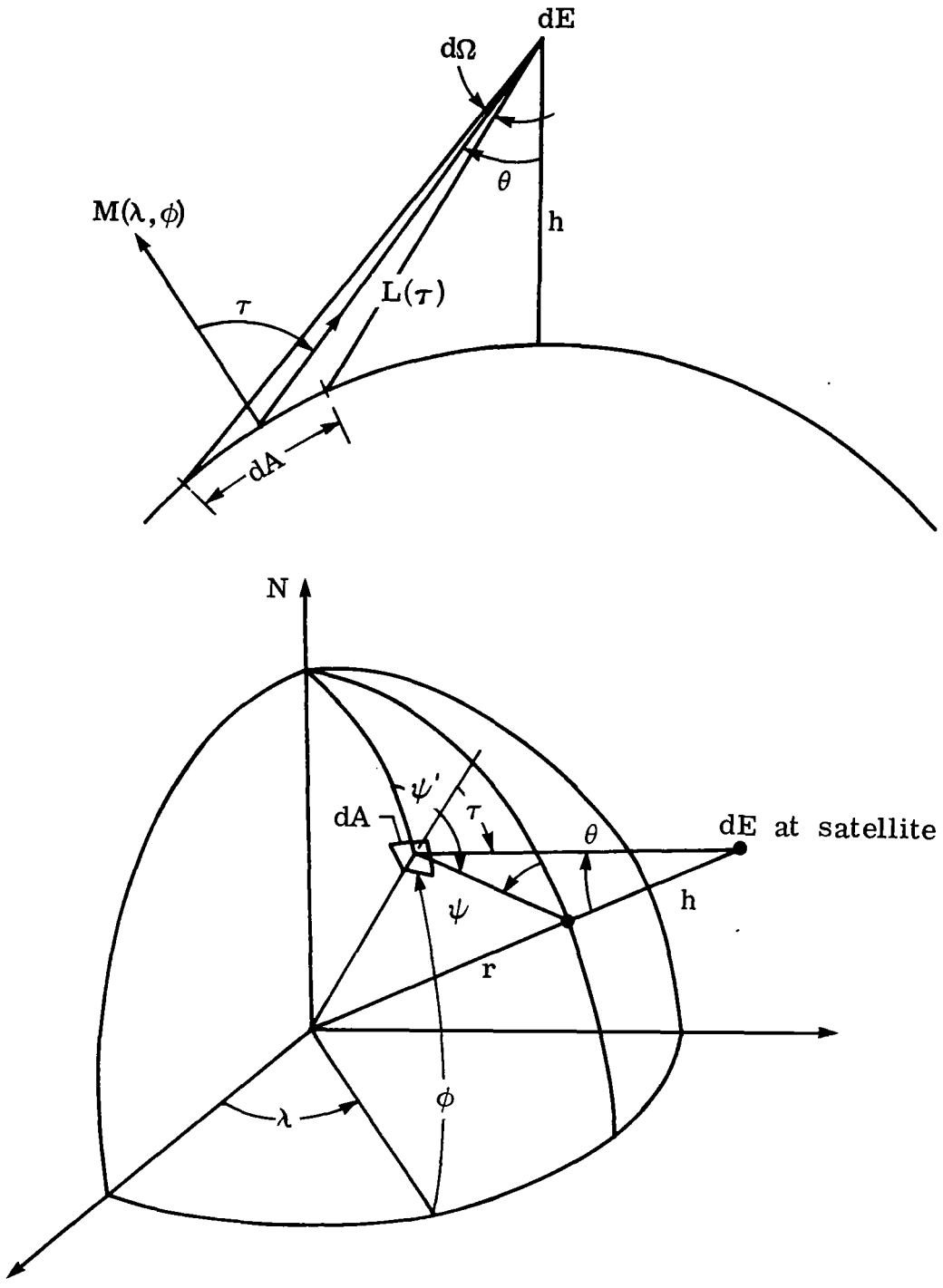

Figure 1.- Geometry of wide-field-of-view radiometer measurement.

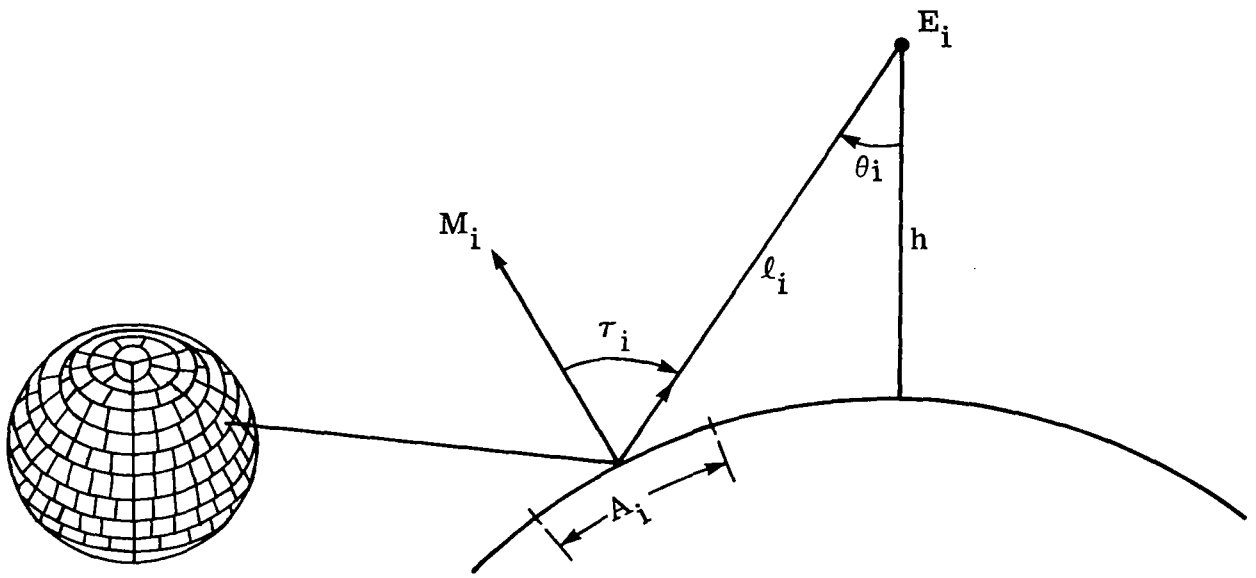

Figure 2.- Geometry of simulated irradiance measurement and flux density model.

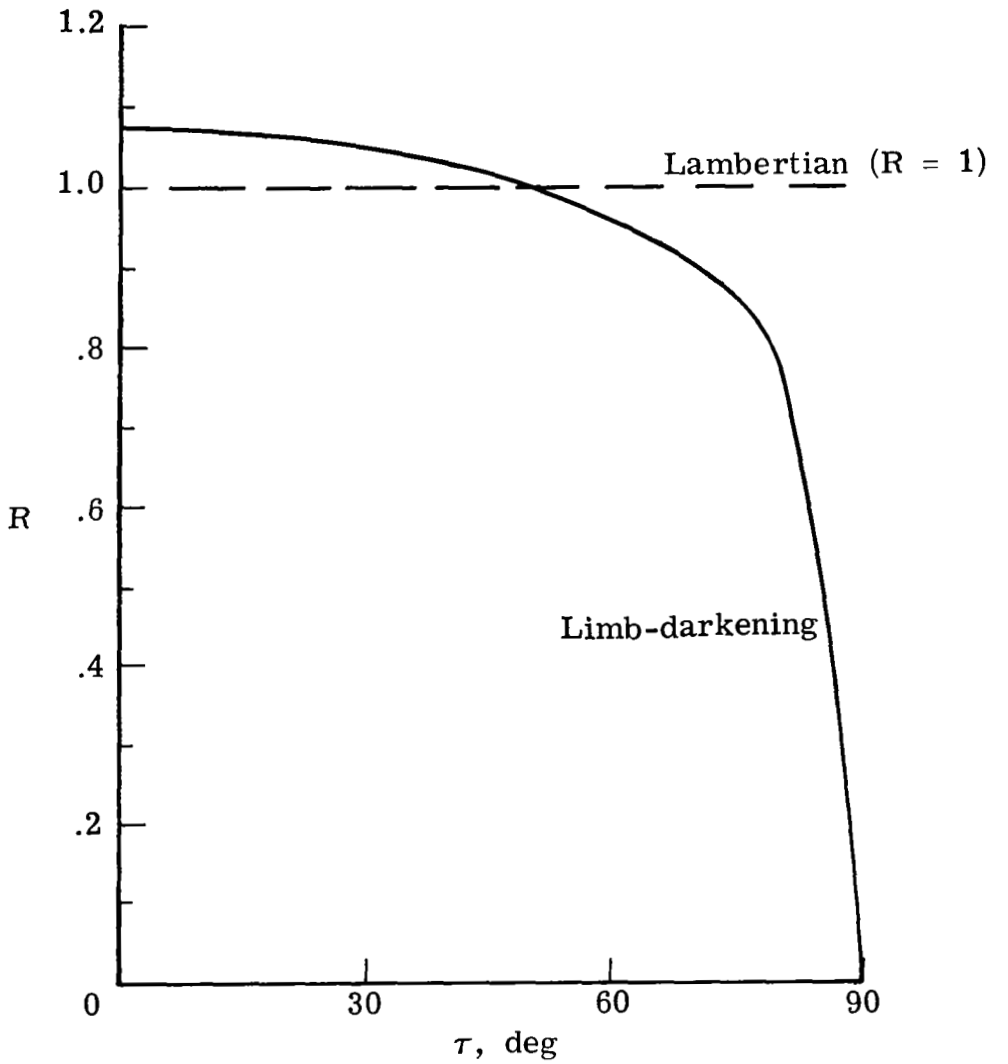

Figure 3.- Lambertian and limb-darkening function for radiation model.

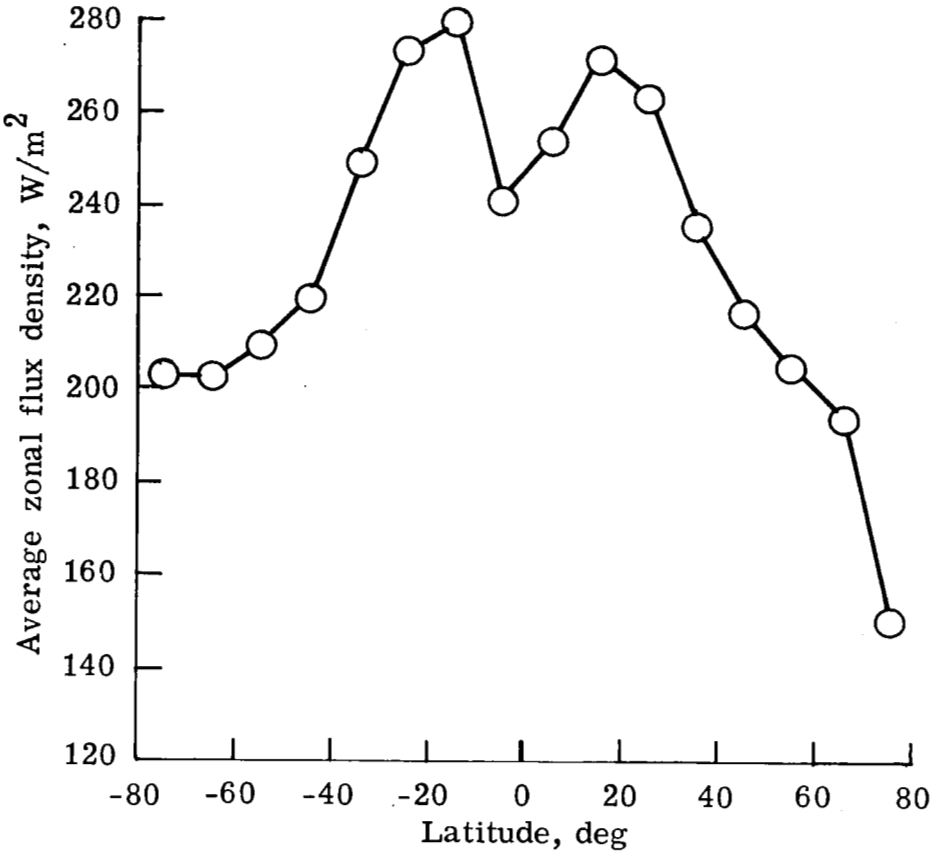

Figure 4.- Reference flux densities from radiation model. Global flux density, 239.53 W/m^2.

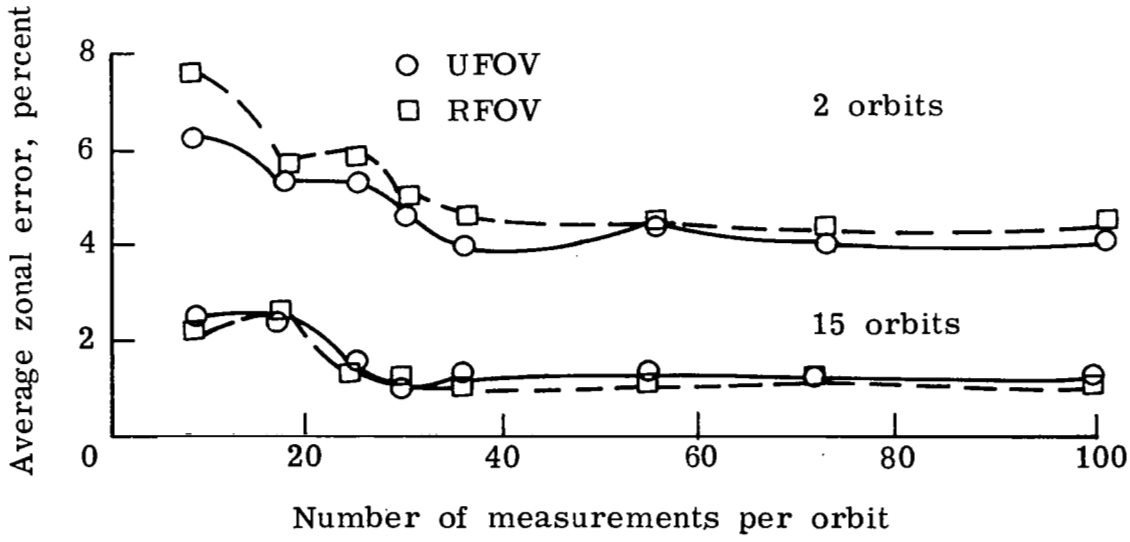

Figure 5.- Effect on AZE of number of orbits and number of measurements per orbit for UFOV and RFOV flat-plate detectors. Lambertian model; h = 600 km.

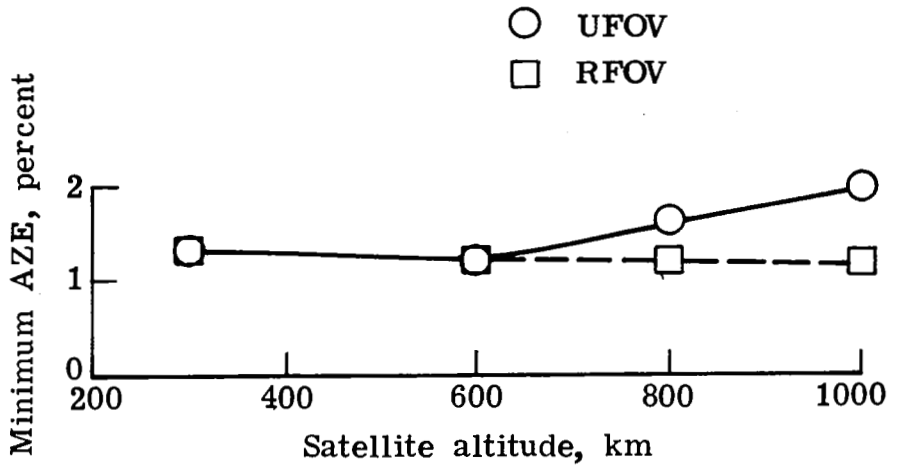

Figure 6.- Effect on minimum AZE of orbit altitude for UFOV and RFOV flat-plate detectors and Lambertian radiation model.

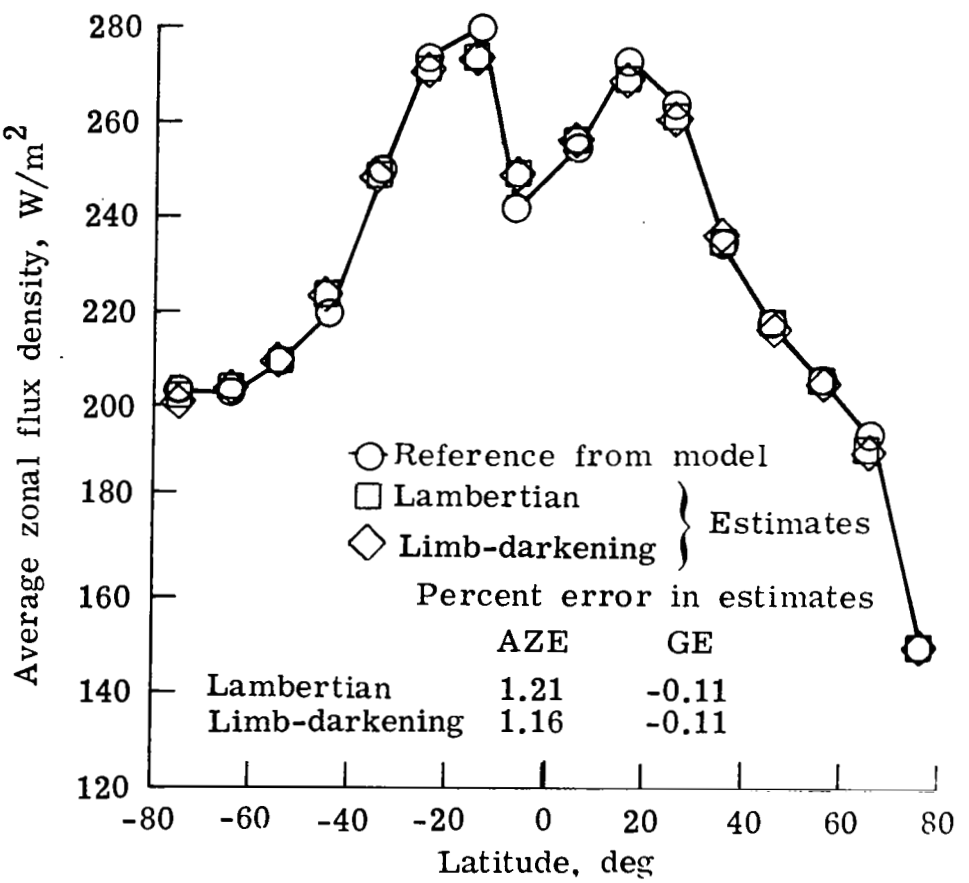

Figure 7.- Estimated and reference values of zonal and global flux density with UFOV flat-plate detectors.

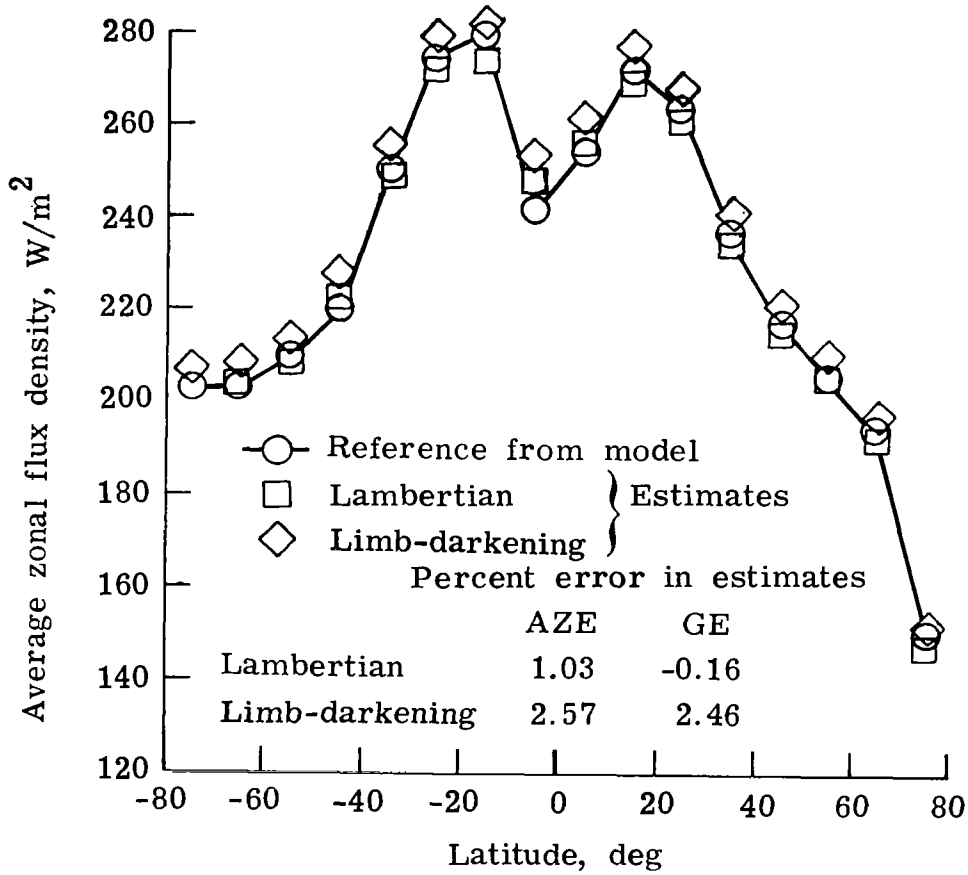

Figure 8.- Estimated and reference values of zonal and global flux density with RFOV flat-plate detector.

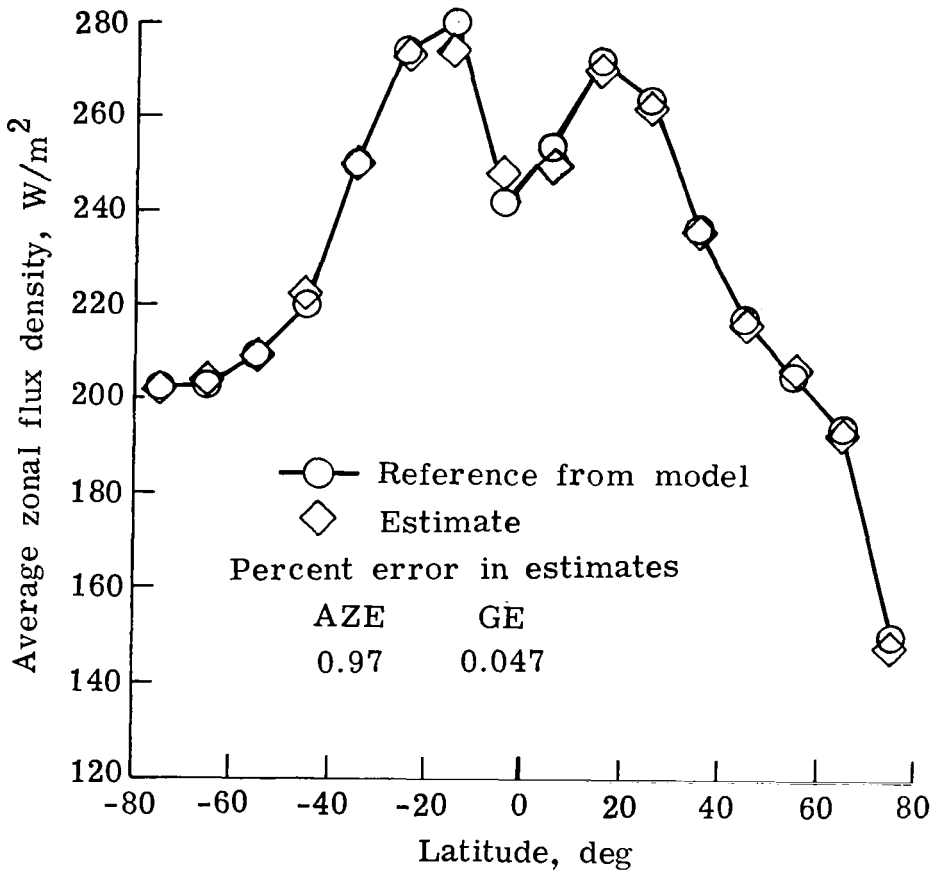

Figure 9.- Estimate of zonal and global flux density based on optimum shape factor for measurements with RFOV flat-plate detector and limb-darkening radiation model.

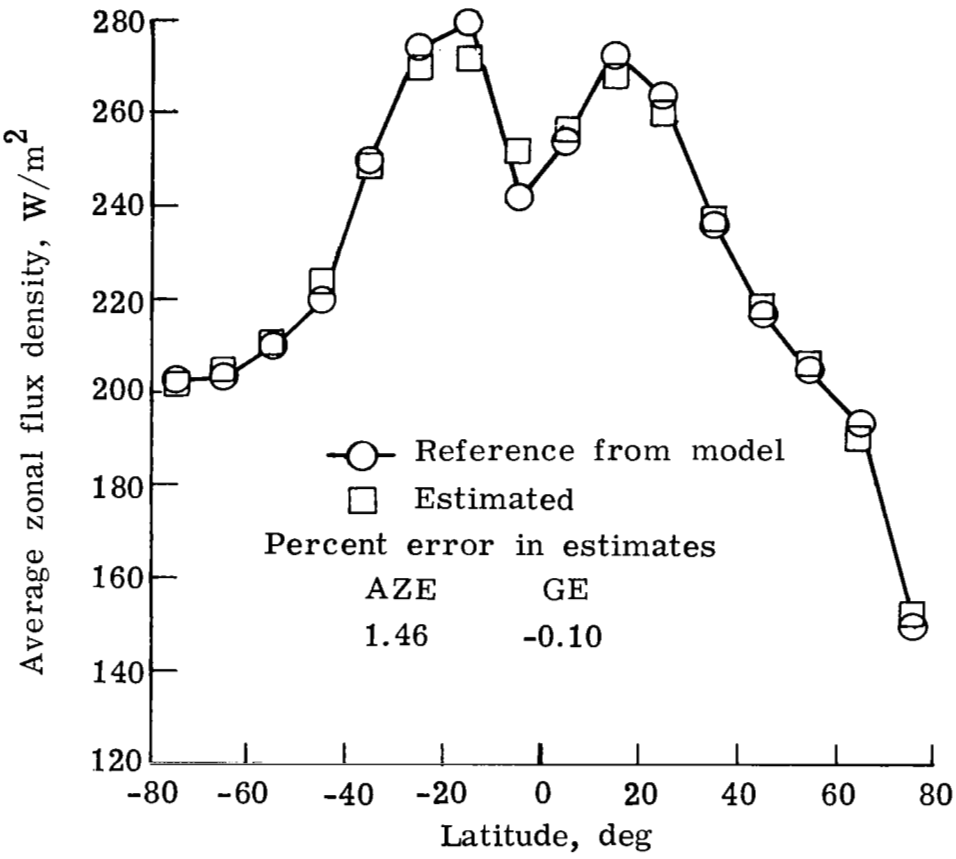

Figure 10.- Estimated and reference values of zonal and global flux density with a spherical detector and Lambertian model. 15 orbits; 72 measurements per orbit; altitude, 600 km.

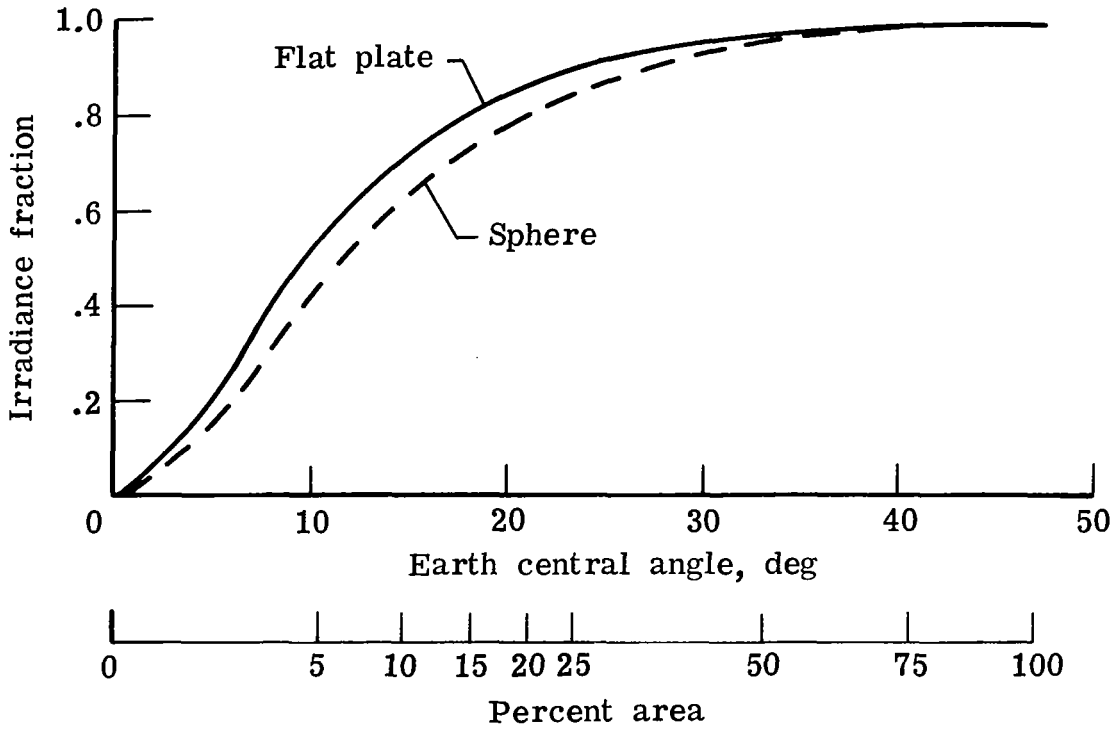

Figure 11.- Irradiance fraction for UFOV flat-plate and spherical detectors at an altitude of 600 km.

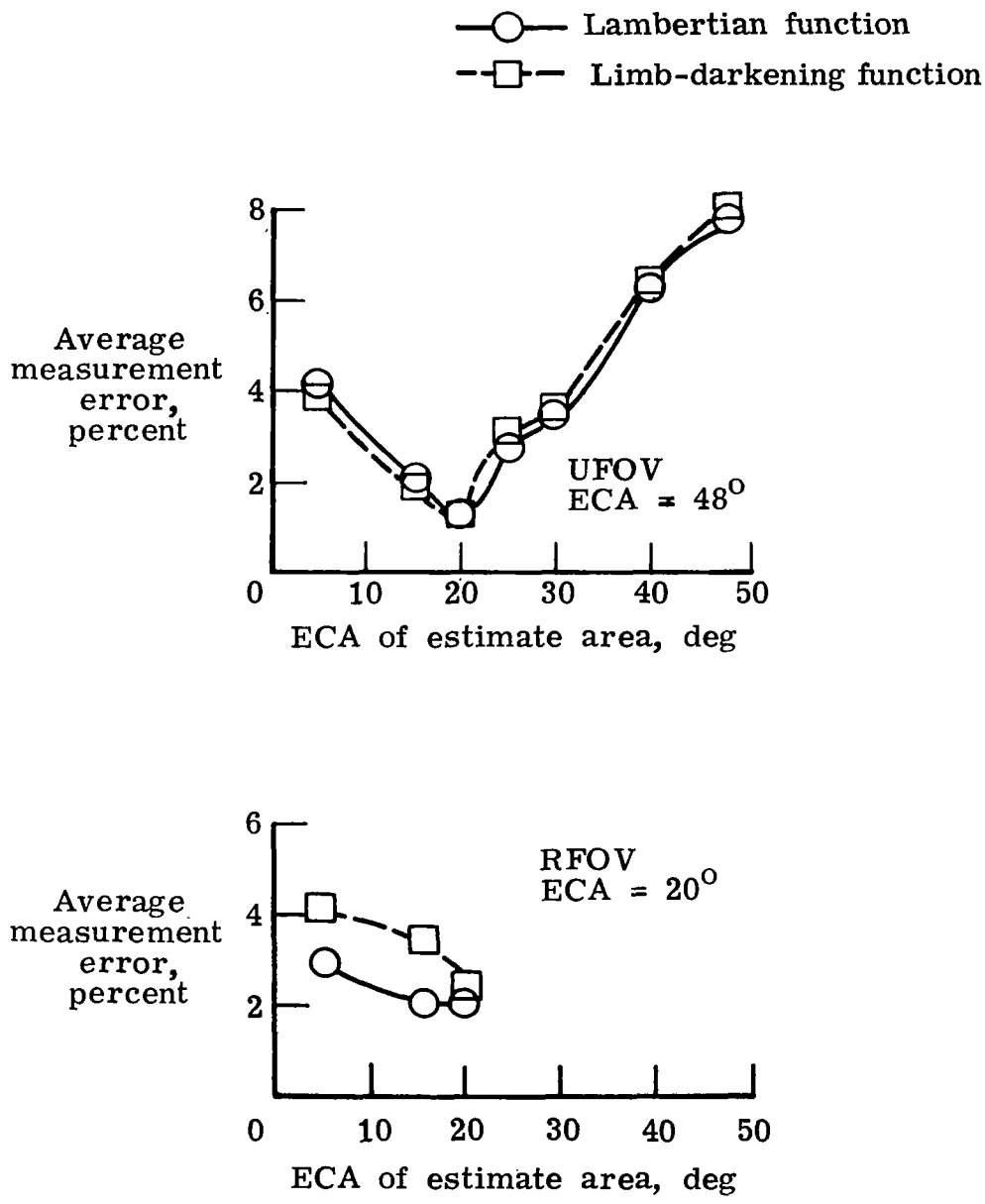

Figure 12.- Average measurement errors for UFOV and RFOV flat-plate detectors at an altitude of 600 km.

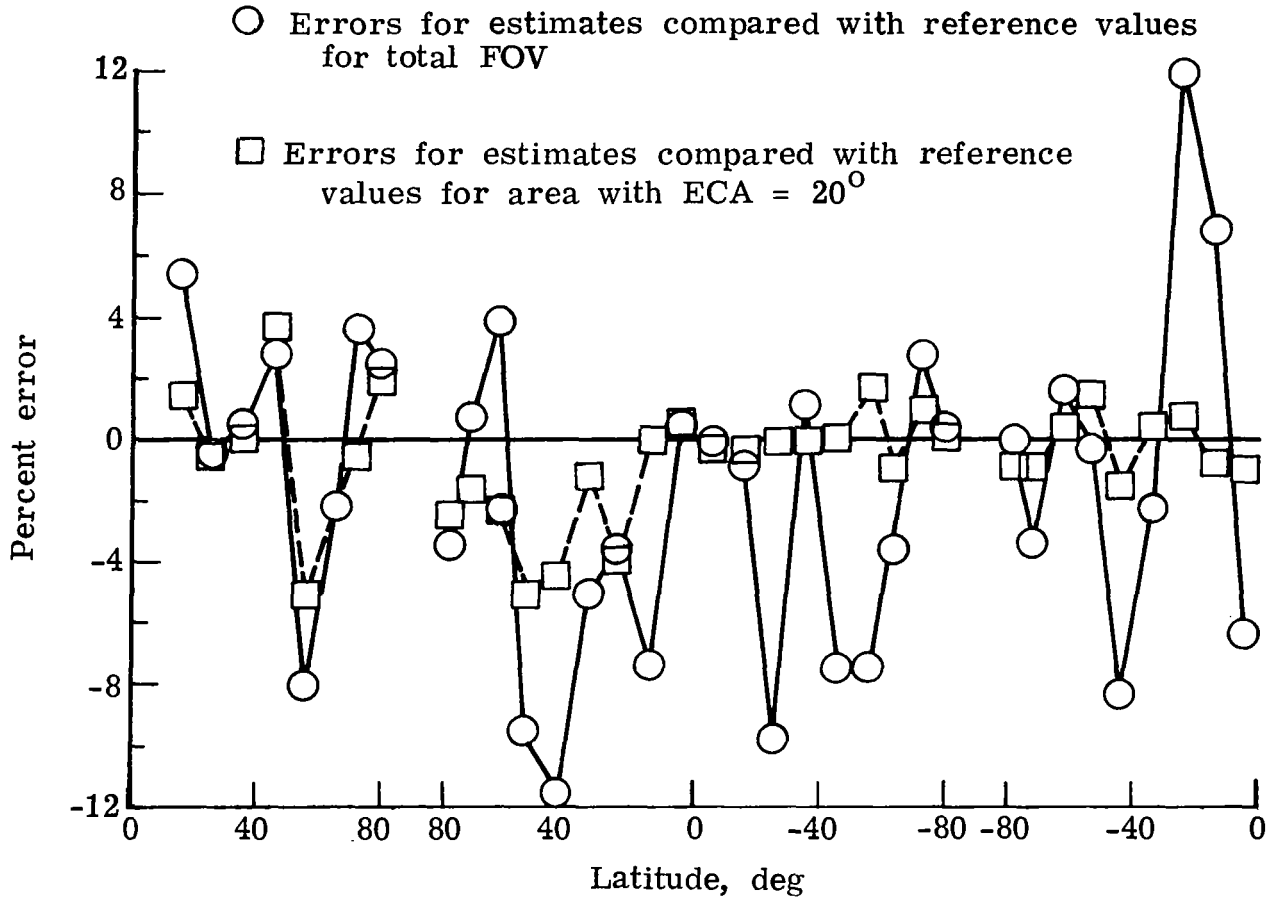

Figure 13.- Errors in estimating flux densities for individual measurements with UFOV detector at an altitude of 600 km.

1. Report No.	2. Government Accession No.	3. Recipient's Catalog No.
NASA TP-1629		

4. Title and Subtitle	5. Report Date
SIMULATION STUDY OF A GEOMETRIC SHAPE FACTOR TECHNIQUE FOR ESTIMATING EARTH-EMITTED RADIANT FLUX DENSITIES FROM WIDE-FIELD-OF-VIEW RADIATION MEASUREMENTS	April 1980
	6. Performing Organization Code
7. Author(s)	8. Performing Organization Report No.
William L. Weaver and Richard N. Green	L-13373
	10. Work Unit No.
9. Performing Organization Name and Address	619-12-01-02
NASA Langley Research Center Hampton, VA 23665	11. Contract or Grant No.
	13. Type of Report and Period Covered
12. Sponsoring Agency Name and Address	Technical Paper
National Aeronautics and Space Administration Washington, DC 20546	14. Sponsoring Agency Code

15. Supplementary Notes

16. Abstract

A study was performed in which geometric shape factors were computed and applied to satellite-simulated irradiance measurements to estimate Earth-emitted flux densities for global and zonal scales and for areas smaller than the detector field of view (FOV). Wide-field-of-view flat-plate detectors were emphasized, but spherical detectors were studied. The radiation field was modeled after data from the Nimbus 2 and 3 satellites. At a satellite altitude of 600 km, zonal estimates were in error 1.0 to 1.2 percent and global estimates were in error less than 0.2 percent. Estimates with unrestricted-field-of-view (UFOV) detectors were about the same for Lambertian and limb-darkening radiation models. The opposite was found for restricted-field-of-view detectors. UFOV detectors are poor estimators of flux density from the total FOV and are much better as estimators of flux density from a circle centered at the FOV with an area significantly smaller than that for the total FOV.

17. Key Words (Suggested by Author(s))	18. Distribution Statement
Earth radiation budget Simulation Emitted radiation Wide-field-of-view radiometers	Unclassified - Unlimited Subject Category 47

19. Security Classif. (of this report)	20. Security Classif. (of this page)	21. No. of Pages	22. Price*
Unclassified	Unclassified	26	$4.50

* For sale by the National Technical Information Service, Springfield, Virginia 22161

NASA-Langley, 1980